Supplementary Information

Intercalation of alkylamines in layered MoO_3 and *in-situ* carbonization for high-performance asymmetric supercapacitor

Ningna Chen,[a] Lu Ni,[a] Jinhua Zhou,[a] Guoyin Zhu,[a] Yu Zhang,[a] Shanyong Chen,[a] Fujie Gao,[a] Chunliang Lu,[b] Hongmei Ji,[c] Jing Chen,[d] Xizhang Wang,[a] Xuefeng Guo,[a] Luming Peng,[a] Weiping Ding,[a] Wenhua Hou [a,*]

a. Key Laboratory of Mesoscopic Chemistry of MOE, School of Chemistry and Chemical Engineering, Nanjing University, Nanjing 210023, P. R. China.
b. Analytical Testing Center, Yangzhou University, Yangzhou 225009, P. R. China.
c. Jiangsu Laboratory of Advanced Functional Materials, Department of Chemistry, Changshu Institute of Technology, Changshu 215500, P. R. China.
d College of Chemistry and Molecular Engineering, Nanjing Tech University, Nanjing 211816, P. R. China.

* Corresponding author. E-mail: whou@nju.edu.cn; Tel: (+86)-25-89686001

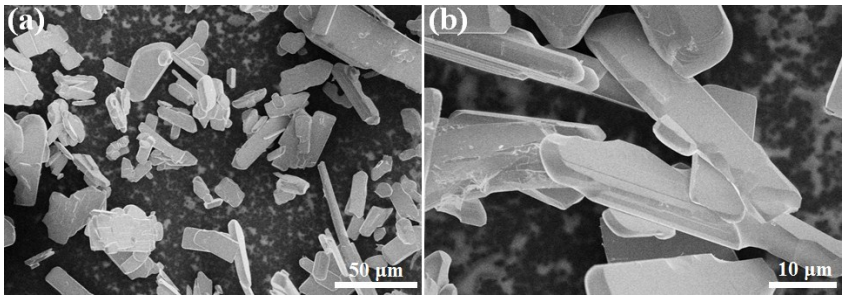

Fig. S1 SEM images of MoO_3 at different magnifications.

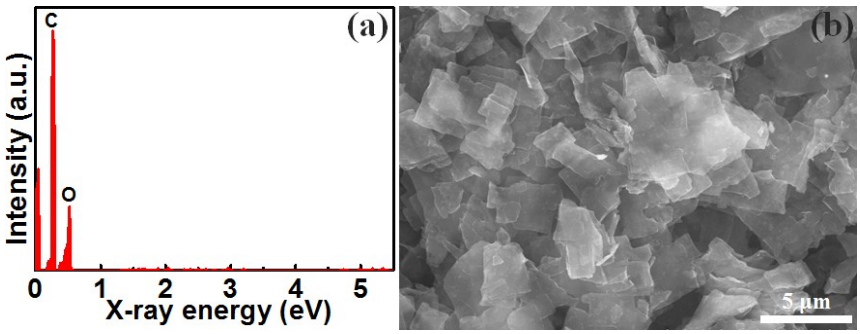

Fig. S2 (a) EDX spectrum and (b) SEM image of the interlayered carbon obtained by dissolving MoO_3/C_{HDA} in 2 mol·L^{-1} NaOH solution to eliminate host MoO_3 layers.

As seen from Fig. S3a and b, the raw MoO_3 presents the well-defined (010) crystal planes with a narrow interlayer spacing about 0.69 nm, showing the typical layered structure. After introduction of DA, the interlayer spacing of (010) crystal planes is significantly increased to ~2.65 nm, further demonstrating the successful intercalation of alkylamines (Fig. S3c and d). A final calcination of MoO_3/DA leads to the formation of sandwich-like MoO_3/C_{DA} hybrid nanostructures (Fig. S3e and f).

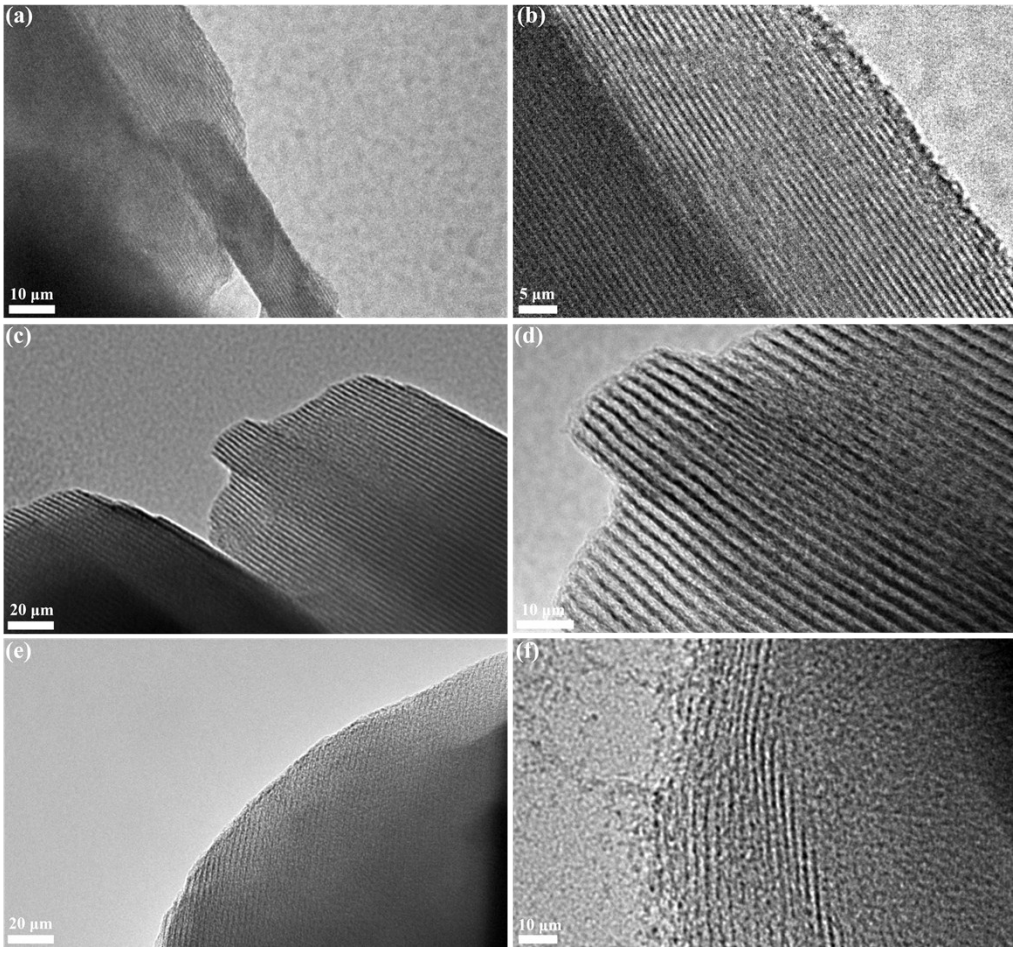

Fig. S3 HRTEM images of MoO_3 (a, b), MoO_3/DA (c, d) and MoO_3/C_{DA} (e, f).

According to the Eq.1 as following:

$$i = av^b \qquad (1)$$

where i is the current, v is the scan rate, and both a and b are the constant parameters, the b value can be determined as a slope of the linear plot between log i vs. log v. Typically, the b value is equal to 1.0 for non-diffusion-controlled surface capacitive and 0.5 for diffusion-controlled redox reaction.

As shown in Fig. S4a, the fitting results show that the b values in this work are 0.89 and 0.93 at the potentials of 0.08 and 0.49 V, respectively. It further confirms that the MoO_3/C_{DA} has both EDLC and surface redox reactions.

In addition, the contribution of the intercalation capacitance can be calculated based on Eq. 2:

$$i\,(V) = k_1 v + k_2 v^{1/2} \qquad (2)$$

where $k_1 v$ and $k_2 v^{1/2}$ correspond to the surface capacitive current and diffusion-

controlled current, respectively. By plotting $i/v^{0.5}$ vs. $v^{0.5}$, k_1 and k_2 can be determined as the slope and intercept, respectively (Fig. S4b).

Fig. S4c shows the percentage of intercalation capacitive at different scan rates and it can be found that the intercalation capacitance decreases as the scan rate is increased due to the diffusion limit of the electrolytes.

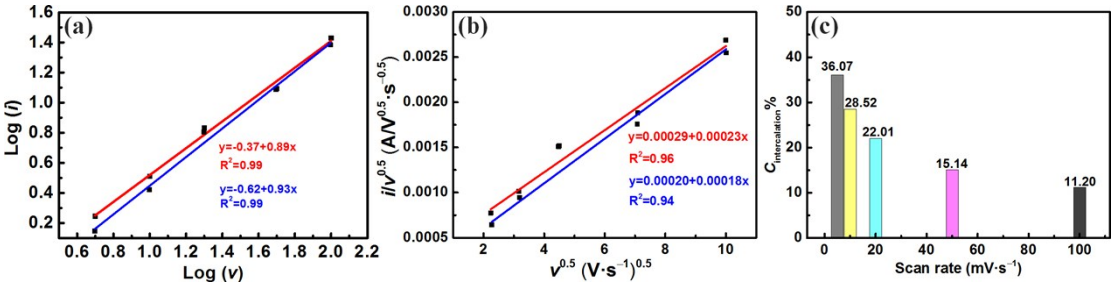

Fig. S4 (a) log *i vs.* log *v*, (b) $i/v^{0.5}$ vs. $v^{0.5}$, and (c) a bar chart of the diffusion-controlled intercalation capacitance vs. scan rate of MoO_3/C_{DA}.

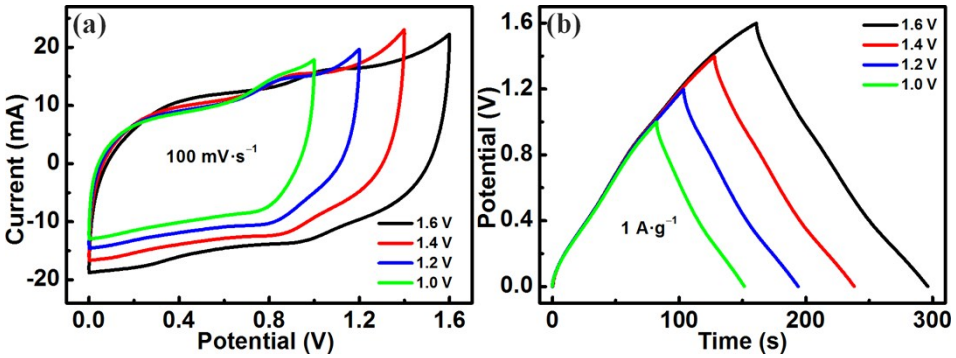

Fig. S5 (a) Cyclic voltammetry curves of MoO_3/C_{DA}//EG asymmetric supercapacitor at increasing voltage window from 1.0 V to 1.6 V (all acquired at 100 $mV \cdot s^{-1}$) and (b) Corresponding galvanostatic charge-discharge curves at a current density of 1.0 $A \cdot g^{-1}$ from 1.0 V to 1.6 V.

Table S1 XPS peak fitting results for MoO_3/C_{PA} (a), MoO_3/C_{DA} (b) and MoO_3/C_{HDA} (c) in the Mo 3d region.

(a)	Peak	Position (eV)	Relative peak area (%)	FWHM (eV)
	$Mo^{4+}(3d_{5/2})$	228.8	24.2	1.6
	$Mo^{4+}(3d_{3/2})$	233.1	4.3	2.1
	$Mo^{6+}(3d_{5/2})$	231.6	55.2	2.0
	$Mo^{6+}(3d_{3/2})$	234.6	16.3	1.0
(b)	Peak	Position (eV)	Relative peak area (%)	FWHM (eV)
	$Mo^{4+}(3d_{5/2})$	228.8	30.9	1.6
	$Mo^{4+}(3d_{3/2})$	233.1	7.3	2.2
	$Mo^{6+}(3d_{5/2})$	231.6	46.3	2.1
	$Mo^{6+}(3d_{3/2})$	234.7	15.5	2.0
(c)	Peak	Position (eV)	Relative peak area (%)	FWHM (eV)
	$Mo^{4+}(3d_{5/2})$	228.8	20.3	2.0
	$Mo^{4+}(3d_{5/2})$	233.1	8.8	2.0
	$Mo^{6+}(3d_{5/2})$	231.5	48.4	1.7
	$Mo^{6+}(3d_{3/2})$	234.6	22.5	1.5

Table S2 XPS peak fitting results for MoO_3/C_{PA} (a), MoO_3/C_{DA} (b) and MoO_3/C_{HDA} (c) in the C 1s region.

(a)	Peak	Position (eV)	Relative peak Area (%)	FWHM (eV)
	Mo–C	283.3	18.7	1.0
	C–H	283.8	59.8	1.4
	Intercalated C	285.3	21.5	1.9
(b)	Peak	Position (eV)	Relative peak Area (%)	FWHM (eV)
	Mo–C	283.5	21.2	1.1
	C–H	284.4	49.0	1.1
	Intercalated C	285.3	29.8	1.9
(c)	Peak	Position (eV)	Relative peak Area (%)	FWHM (eV)
	Mo–C	284.0	10.5	0.9
	C–H	284.5	61.3	1.2
	Intercalated C	286.1	28.2	1.9

Table S3 A comparison of specific capacitance, rate capability and cycle stability of the present work with those reported MoO_3-based asymmetric supercapacitor.

ASC	Capacitance	Rate capability	Cycling performance	Ref
MoO_3/C_{DA}//EG	88 $F\cdot g^{-1}$ (1 $A\cdot g^{-1}$)	69.3% (1 to 10 $A\cdot g^{-1}$)	86.5% (1 $A\cdot g^{-1}$ for 5000 cycles)	This work
MoO_3//AC	68 $F\cdot g^{-1}$ (1 $A\cdot g^{-1}$)	20.7% (0.5 to 10 $A\cdot g^{-1}$)	113% (2 $A\cdot g^{-1}$ for 10000 cycles)	1
MoO_3–PPy//CNTs–MnO_2	54 $F\cdot g^{-1}$ (0.25 $A\cdot g^{-1}$)	/	76% (5 $A\cdot g^{-1}$ for 10000 cycles)	2
WO_{3-x}/MoO_{3-x}// PANI/carbon	216 $mF\cdot cm^{-2}$ (2 $mA\cdot cm^{-2}$)	60.2% (2 to 20 $A\cdot g^{-1}$ $mA\cdot cm^{-2}$)	75% (5 $mA\cdot cm^{-2}$ for 10000 cycles)	3
CF/MnO_2//CF/MoO_3	4.86 $mF\cdot cm^{-2}$ (0.5 $mA\cdot cm^{-2}$)	65.8% (0.5 to 5 $mA\cdot cm^{-2}$)	89% (5 $mA\cdot cm^{-2}$ for 3000 cycles)	4
MnO_2@TiN//N-MoO_{3-x}	10.3 $mF\cdot cm^{-1}$ (0.25 $mA\cdot cm^{-1}$)	/	80.3% (100 $mV\cdot s^{-1}$ for 5000 cycles)	5

Reference

1 F. Barzegar, A. Bello, D. Y. Momodu, J. K. Dangbegnon, F. Taghizadeh, M. J. Madito, T. M. Masikhwa and N. Manyala, *RSC Adv.*, 2015, **5**, 37462-37468.

2 P. Du, W. Wei, D. Liu, H. Kang, C. Liu and P. Liu, *J. Mater. Sci.*, 2018, **53**, 5255-5269.

3 X. Xiao, T. Ding, L. Yuan, Y. Shen, Q. Zhong, X. Zhang,Y. Cao, B. Hu, T. Zhai, L. Gong, J. Chen, Y. Tong, J. Zhou and Z. Wang, *Adv. Energy Mater.*, 2012, **2**, 1328-1332.

4 J. Noh, C. Yoon, Y. Kim, J. Jang, *Carbon,* 2017, **116**, 470-478.

5 M. Yu, X. Cheng,Y. Zeng, Z. Wang,Y. Tong, X. Lu and S. Yang, *Angew.Chem.,* 2016, **128**, 6874 - 6878.